Design of novel molecular wires for realizing long-distance electron transfer

Albers, W.M.; Lekkala, J.O.; Jeuken, L.; Canters, G.W.; Turner, A.P.F.

ELSEVIER

Bioelectrochemistry and Bioenergetics 42 (1997) 25–33

BIOELECTROCHEMISTRY and BIOENERGETICS

Design of novel molecular wires for realizing long-distance electron transfer

Willem M. Albers [a,*], Jukka O. Lekkala [a], Lars Jeuken [b], Gerard W. Canters [b], Anthony P.F. Turner [c]

[a] *VTT Chemical Technology, Materials Technology, Sensor Materials, P.O. Box 14021, FIN-33101 Tampere, Finland*
[b] *Gorlaeus Laboratories, Leiden Institute of Chemistry, Leiden University, P.O. Box 9502, 2300 RA Leiden, The Netherlands*
[c] *Cranfield Biotechnology Centre, Cranfield University, Cranfield, Beds. MK43 0AL, UK*

Received 14 June 1996; accepted 21 August 1996

Abstract

Novel heteroarene oligomers, consisting of two pyridinium groups, linked by thiophene units of variable length, "thienoviologens", are described as promising candidates for molecular wires. Two representative thienoviologens were coated by adsorption from micromolar concentrations in ethanol onto octadecylmercaptan (ODM)-coated gold electrodes and induced a gradual restoration of the electrochemistry with hexacyanoferrate as a function of molecular wire concentration. Glucose oxidase and choline oxidase showed strong adsorption to these conductive layers, but showed striking differences in adsorption to the different thienoviologen layers. The measurements support the hypothesis that the molecules are incorporated in the ODM layer in a different fashion. Also the complex formation of an engineered azurin redox protein with water-soluble pyridyl ligands is presented in relation to a possible application of the thienoviologens as conductive spacers, in which the contact with the redox protein is achieved via complex formation with a free pyridine nitrogen. © 1997 Elsevier Science S.A.

Keywords: Molecular wires; Electron transfer; Heteroarene oligomers; Thienoviologens

1. Introduction

The application of new conductive materials for the attainment of electronic communication between redox enzymes and electrode surfaces is one of the topics within biosensor research which has received steadily growing attention over the past 12 years. A large number of electron-conductive materials have been studied in the construction of amperometric enzyme electrodes [1–3]. New molecular conductors, as developed in the field of molecular electronics, can be considered as the most promising components. In principle, effective electron transfer can be achieved with molecular wires which form a permanent conductive bridge between the enzyme and the electrode [4]. Such wires should be able to cross distances ranging from 20 Å to 50 Å, which is the typical size of a protein molecule or biological membrane. Basic examples of molecular wires, designed to work in biomembranes, are the caroviologens, described by Arrhenius et al. [5] and the bipyridyl-linked metal complexes reported by Launey et al. [6].

In the present work molecular wires are reported, consisting of an oligothiophene conducting spacer of variable length terminated by pyridine or pyridinium substituents. These acceptor–donor–acceptor (ADA)-type molecular wires are designated as thienoviologens in analogy with the caroviologens. The shortest thienoviologens, with one central thiophene, are known to form stable radical monocations with strong absorptions in the near-infrared region [7]. The thienoviologens are also highly fluorescent [8] and the insertion of additional thiophene units in the chain causes moderate bathochromic shifts for each inserted thiophene unit [9]. Additionally, thienoviologens are known for their electrochromic properties [10] and thus may prove to have great utility as opto-electronic transducing materials.

The insertion of thienoviologens in electronically insu-

* Corresponding author. Tel: +358 31 3163 318; fax: +358 31 3183 319.

PII S0302-4598(96)05150-1

lating monomolecular layers was the primary objective of our initial investigations. In this respect, self-assembly provided a convenient method to prepare thienoviologen-modified electrode surfaces. Self-assembly is a process that generally involves low concentrations (micromolar to millimolar) of a suitable molecule being adsorbed onto a surface over extended periods of time (12–48 h) [11]. The self-assembly method generally allows for versatility in coating conditions and changing the components on the surface and is experimentally easily performed when some critical factors are taken into account. In this study the thienoviologens were adsorbed using similar procedures, but a study of molecular ordering was not yet undertaken.

The association of redox proteins with self-assembled organic layers has been subject of intensive study since the discovery by Eddowes and Hill that 4,4′-bipyridyl, self-assembled on gold electrodes, enabled efficient electron transfer from cytochrome c [12]. Many types of surface modifiers for gold, including several π-bridged 4,4′-bipyridyls, were described by Allen et al. as being highly effective in promoting cytochrome c electrochemistry [13]. The proposed prerequisites for successful electron transfer with this system was the possibility to form weak, reversible binding between the protein and the surface, as mediated by complementary electrostatic bonds. In a more recent study, by Sagara et al., it was found that the mode of electron transfer may be different for different surface modifiers, depending on the strength with which the modifier is bound to the gold surface [14]. Thus, 4-mercaptopyridine and bis(4-pyridyl)disulfide were observed to bind most tightly to gold, enabling tight binding of the cytochrome c without denaturation, while 4,4′-bipyridyl was less strongly bound and showed competitive binding with cytochrome c to gold. In the latter case the protein may become partially denatured. Finally, 1,2-bis(4-pyridyl)ethylene did not adsorb to gold strongly enough to compete with cytochrome c and bare protein adsorbed to the gold surface in a denatured state. A more basic understanding of how enzymes are adsorbed to the formed layers as a function of coating conditions is an important step on the route to functional enzyme electrodes. Thus, the adsorption of two model enzymes on two types of substrates was investigated, using a broad range of enzyme concentrations. Particularly glucose oxidase (GOx) has been used in most studies that deal with amperometric biosensors, since it has many favourable properties [15]. In a recent study by Willner et al., GOx was adsorbed to self-assembled layers of 1-(4-mercaptobutyl)-3,3-dimethyl-6′-nitrospiro[indolin-2,2′-[1-2*H*]benzopyran] (SP) on gold [16]. SP is a photoswitchable dye compound, which can be reversibly converted into a nitromerocyanine dye (MRH^+) by UV light irradiation. It was observed that GOx adsorbed more strongly to the thin film in the MRH^+ state, as evidenced by quartz crystal microbalance measurements. This may indicate a reinforcement of the electrostatic interaction between the photochemically introduced positive charge in the film with the strongly negatively charged GOx. The electron transfer rate, in the presence of ferrocene carboxylic acid as a mediator, appeared to decrease from 4.7×10^{-2} to 5.6×10^{-3} cm s^{-1}. This may primarily be due to electrostatic repulsion between the ferrocene carboxylic acid and the MRH^+ film. In contrast, the electron transfer rate of GOx covalently modified with ferrocene showed an almost two-fold increase when the film was switched from SP the MRH^+. Thus, among other factors, careful control over the amount of positive charges on the surface may be desirable in optimising the activity of the bound GOx.

A particularly interesting application of oligomeric bi(4-pyridyl)thiophene spacers would be to insert the pyridine moiety into a recognition site of a redox protein, in order to anchor the protein to an electrode surface or to a bilayer in which the spacer is embedded [4]. As a test case we have used an engineered blue copper protein, azurin from *Pseudomonas aeruginosa*, in which the active site has been made accessible from the outside by the creation of a channel leading to the copper redox centre. We were interested to see if pyridine ligands would bind effectively to the modified Cu site of the His117Gly azurin mutant. To this end we selected two easily soluble pyridines, 3-(3-pyridyl)-propanol and 3-(4-pyridyl)-propanol, and studied their binding to the azurin mutant.

2. Materials and methods

2.1. Synthesis of thienoviologens

Cross-coupling of Grignard, organotin or organozinc reagents with haloarenes, in the presence of nickel or palladium phosphine catalysts, has become the method of choice for the preparation of complex heteroarene oligomers in high yield [17]. Recently, different extended di(4-pyridyl)thiophene oligomers have been prepared by Japanese researchers by a Busch-type reaction, involving palladium amalgam as the catalyst in the presence of hydrazine [8]. An alternative synthesis of a series of extended di(4-pyridyl)thiophene oligomers, containing up to five thiophenes between two terminal 4-pyridine groups, has been previously reported by our group [18]. The compounds could be produced effectively by the cross-coupling of α-dibrominated thiophene oligomers with the organozinc derivative of 2-(4-pyridyl)thiophene using 1,1′-bis(diphenylphosphinoferrocene) palladium(II) dichloride, $Pd(dppf)Cl_2$, as a catalyst. The di(4-pyridyl)thiophene oligomers can be subsequently alkylated or modified by complex formation with different metals (Zn, Cu, Ru, Os). Methylation with methyl iodide readily produced methyl thienoviologens [8,9,18]. Scheme 1 presents the synthetic routes for PT2 and PT3, the molecules compared in the present study.

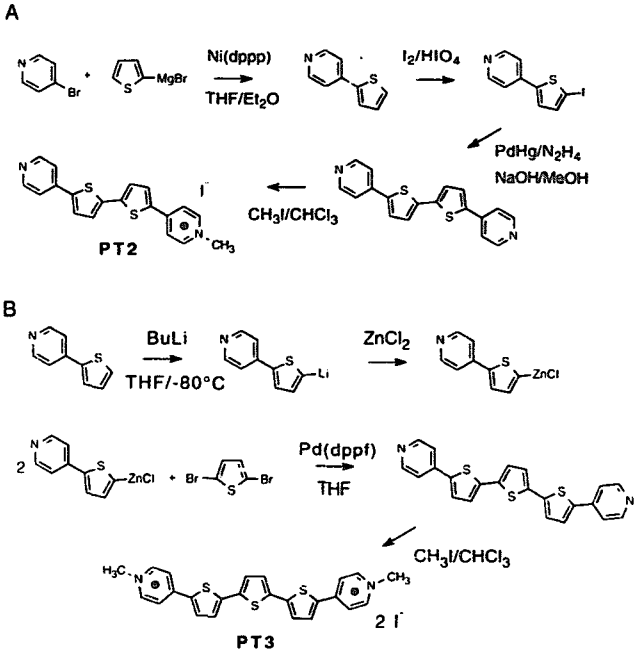

Scheme 1.

2.2. Electrode coating

Miniature three-electrode systems, containing a gold working electrode, a silver reference electrode and a platinum counter electrode, were patterned on glass or silicon dioxide substrates by the lift-off technique. The working electrode (Au) had a geometric surface area of 9 mm^2. In other types of coating studies, where no electrochemical tests were required, gold was sputtered on silicon wafers, which were subsequently cut into rectangular pieces of 6×9 mm^2. In all cases the adhesion of the gold to the substrate was enhanced by a 10 nm intermediate layer of chromium.

The gold substrates were coated with a layer of octadecylmercaptan (ODM, Aldrich) as follows. The electrodes were cleaned by an r.f. argon plasma for 0.5 min at 0.8 kV and a pressure of 10 mTorr, and thereafter immediately immersed in a coating solution containing 1 mM ODM in ethanol (A.R. Grade, ALKO, Finland). The electrodes were left in the solution for 18 h. The slides were then thoroughly rinsed with ethanol and stored in ethanol until further use. All glassware (except the Pasteur pipettes used for transfering the liquids) had been rigorously cleaned by treatment with piranha solution (30% hydrogen peroxide/concentrated sulphuric acid 1:4 v/v) at 80–100°C. *Piranha is highly reactive to all organic materials and should be handled with extreme care!* After this treatment the glassware was rinsed with water (deionized water delivered by a MilliQ-apparatus, Millipore, USA) and oven-dried at 105°C. The tubes were covered with aluminium foil.

2.3. Impedance measurements

Impedance measurements were carried out using a Hewlett Packard 4195A Network/Spectrum analyzer in the frequency range 10 Hz to 100 kHz. All impedance measurements were performed in an electrolyte solution containing 154 mM sodium chloride, 10 mM *N*-(2-hydroxyethyl)-piperazine-*N'*-(2-ethanesulfonic acid) (HEPES), 0.1 M $K_4Fe(CN)_6$ and 0.1 M $K_3Fe(CN)_6$, buffered to a pH value of 7.00. This electrolyte solution produced an electrochemical impedance modulus at 10 Hz very close to that of the electrolyte (32 Ω). A two-electrode set-up was used, employing a gold counter electrode (surface area, approximately 100 mm^2) with an impedance roughly 10 times smaller than that of an uncoated working electrode.

2.4. Electrochemical measurements

Cyclic voltammetry (CV) of the electrodes was performed with an EG&G PARC Potentiostat/Galvanostat Model 263, using EG&G PARC Model 270 electrochemical software. The buffer for CV measurements consisted of 5 mM $K_4Fe(CN)_6$ in PBS buffer (0.154 M NaCl, 10 mM

KH_2PO_4, pH = 7.5). The gold electrodes were mounted in an EG&G Model K0264 MicroCell using the on-chip counter and reference electrodes. The buffer was purged with nitrogen for 0.5 h to reduce oxygen interference.

2.5. Enzyme immobilization and activity assay

The enzymes glucose oxidase, GOx, [EC 1.1.3.4], 149 U mg^{-1} (Fluka) and choline oxidase, ChOx, [EC 1.1.3.17], 10.6 U mg^{-1} (Fluka), were labeled with ^{125}I, using "IODO-BEADS" (Pierce, Rockford IL, USA). Possible differences in the enzymatic activity compared with unlabeled enzymes was checked, and appeared to be negligible. The initial specific activities of the enzymes were 99.25×10^6 CPM mg^{-1} for GOx and 59.8×10^6 CPM mg^{-1} for ChOx. Radiolabelled GOx was partly mixed with unlabeled GOx (1 : 10), while radiolabelled ChOx was used purely as received.

Enzymes were immobilized by passive adsorption onto the slides by placing the gold chip or electrode with the gold face down in an acrylic block aperture with a 0.5 mm gap. An enzyme solution (30 μl) of appropriate concentration was then injected in the gap between the electrode and the acrylic block with a Hamilton syringe. The enzymes were allowed to adsorb at room temperature for 3 h. Hereafter the chips were transferred to glass test tubes and rinsed with PBS buffer three times, taking care not to allow the chips to dry. The chips and electrodes were then left in buffer and the radioactivity was followed for periods of up to 2 weeks, correcting the CPM values for radioactive decay according to a 61 day half-life of the isotope. Comparison of the residual radioactivity on the chips with the value of the corrected specific activity (in CPM μg^{-1}) yielded the amount of immobilized enzyme.

The activity of the enzymes was determined with a standard spectroscopic method as described by Bergmeyer [19], using azino-bis(ethylbenzothiazoline sulphonic acid) di-ammonium salt, ABTS (Fluka 11557) as the chromophore. The enzymatic activity of the slides was recorded in microtitre plates as absorbance values at 405 nm. The microtitre plates were shaken for 1 h at 25°C prior to reading the absorbance values. The enzymatic activity in units (μmol conversion per minute) were obtained by comparison with a known activity of soluble enzyme under similar assay conditions.

2.6. Titration experiments with His117Gly azurin

The His117Gly mutant of azurin from *Pseudomonas aeruginosa*, was expressed in *E. coli* with methods as described earlier [20]. The azurin was dissolved at typically 75 μM in 20 mM 2-(*N*-morpholino)ethanesulphonic acid (MES) buffer at pH = 6.0. The azurin was stepwise titrated with the appropriate ligand in the concentration range 10–600 μM and the UV–vis spectra at each concentration measured at 25°C with a 1 cm pathlength.

3. Results and discussion

3.1. Conductivity of the self-assembled layers

The impedance spectra of the untreated planar gold electrodes showed resistance values of 30 Ω over the whole frequency range, close to the ambient electrolyte solution resistance at high frequency, when the concentration of hexacyanoferrate(II) and (III) in the measuring buffer was at least 0.1 M. After plasma treatment and subsequent coating with ODM of the electrodes, the impedance modulus |Z| at 10 Hz increased to around 100000 Ω as a result of blocking of the electrochemical reaction of the hexacyanoferrate(II)/(III) couple. The phase-angle shift component (θ) of the impedance showed a minimum at a frequency around 1 kHz, characteristic of largely capacitive properties of the electrode.

When the thienoviologens PT2 or PT3 were adsorbed in a period of 18 h from dilute solutions in ethanol onto thin film gold electrodes, a large decrease of the impedance modulus was observed with increasing concentration, as shown for PT3 in Fig. 1(A). The largest change occurred above 40 μM. The phase component of the impedance gradually shifted to higher frequencies and disappeared (Fig. 1(B)). This behaviour is in agreement with a most basic impedance model, in which the capacitance of the ODM layer, C_{ODM}, the resistance of the molecular wire layer, R_w, and the electrolyte solution resistance, R_e, are coupled as in the substitute circuit depicted in Fig. 2.

When the capacitance of the ODM layer is gradually replaced by the resistance of the molecular wire, the impedance of the circuit can be expressed via a variable parameter ϕ, as

$$Z(\phi) = \frac{1}{\left(\frac{\phi}{Z(R_w)} + \frac{(1-\phi)}{Z(C_{ODM})}\right)} + R_e \qquad (1)$$

in which ϕ is a factor between 0 and 1. Since $Z(R_w) = R_w$ and $Z(C_{ODM}) = 1/(j\omega C_{ODM})$, Eq. (1) can be expressed as

$$Z(\phi) = \frac{R_w}{[\phi + (1-\phi)\cdot(j\omega C_{ODM}\cdot R_w)]} + R_e \qquad (2)$$

Non-linear fitting of complex data to the model (Eq. (2)) can be achieved by minimizing the sum (over all frequencies) of the squares of the distance in the complex plane between the observed impedances, Z_{exp}, and the modelled impedances, Z_{est}, using suitable weighting factors [21]. For our data the most consistent results were obtained by minimizing the sum of the residuals relative to the modulus of the observed impedance, according to

$$S_{rel} = \sum_i \left[\left(\frac{|Z_{exp}(\omega_i) - Z_{est}(\omega_i,\phi)|}{|Z_{exp}(\omega_i)|}\right)^2\right] \qquad (3)$$

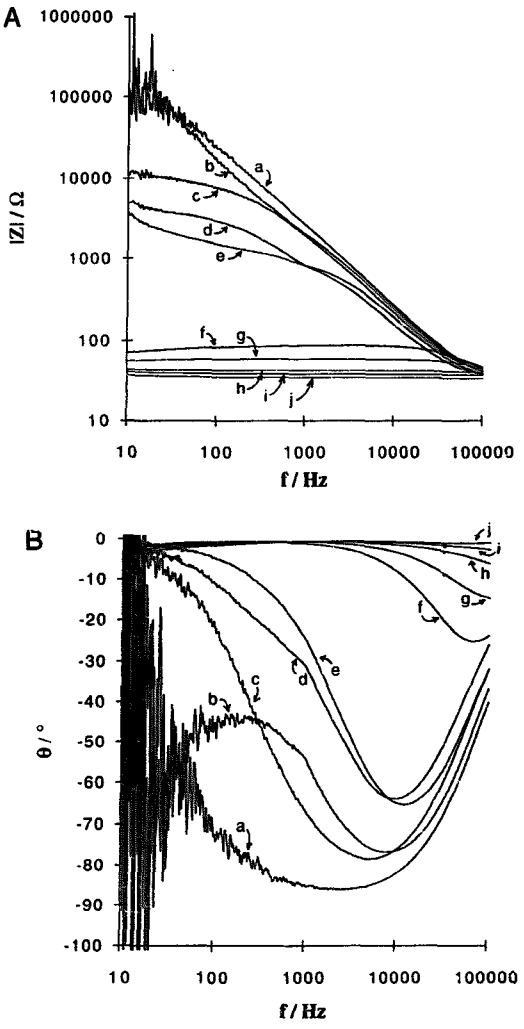

Fig. 1. Impedance spectra of ODM-modified gold electrodes showing the effect of adsorption of PT3 from concentrations of (a) 5, (b) 10, (c) 20, (d) 30, (e) 40, (f) 50, (g) 75, (h) 100, (i) 150 and (j) 200 μM in ethanol. (A) Impedance modulus, $|Z|$; (B) phase shift, θ.

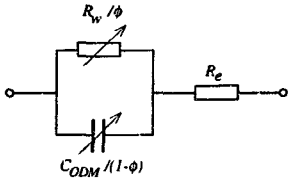

Fig. 2. Impedance model circuit associated with the present monolayer system, containing the capacitance of the insulating ODM layer (C_{ODM}), the resistance of the molecular wire (R_w) and the resistance of the electrolyte solution (R_e). The dimensionless parameter, ϕ, assumes values between 0 and 1, and describes the transition from a capacitive layer to a conductive layer.

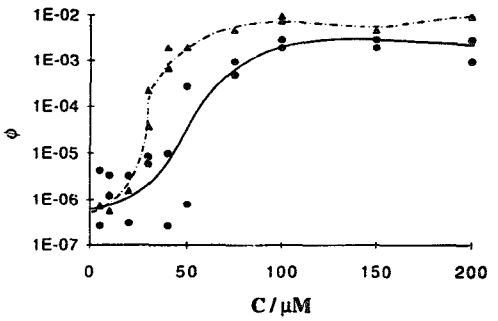

Fig. 3. Change of the parameter, ϕ, with adsorption concentration as obtained from fitted impedance data: for PT2 (– · – ▲ – · –); for PT3 (— —●— —).

Non-linear fitting of the experimental data to Eq. (2) resulted in physically sound and constant values for C_{ODM} (0.5 μF) and R_e (32 Ω). The values of R_w were found to be 0.02 ± 0.01 Ω both for PT2 and PT3. The values of ϕ showed variation from 2.7×10^{-7} to 2×10^{-3} with adsorption concentration as depicted in Fig. 3. The parameter ϕ may thus well be related to the fractional surface coverage of the molecular wire. The appearance of conductivity, as observed in the impedance measurements may be due to a small amount of adsorbed molecular wires, as indicated by the small values for ϕ.

Conductivity changes are also observed in cyclic voltammetry measurements. In Fig. 4 the cyclic voltammograms of a series of electrodes incubated with increasing concentrations of molecular wire are presented. It can be observed that the maximum conductivity is attained at significant higher concentrations of PT3 (100–200 μM) in comparison with the impedance measurements.

Similar layers of ODM and PT2 could be produced on copper electrodes (0.75 mm diameter transformer wire, fused in Teflon FEP tubing), using the same procedure for ODM coating as for the thin-film gold electrodes. A blank copper electrode shows a stripping wave for copper at 110

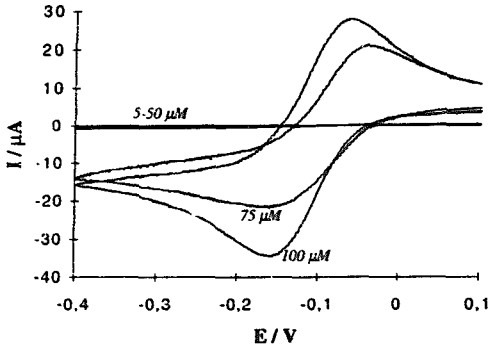

Fig. 4. Change of the cyclic voltammogram of the ODM/Au electrode on adsorption of PT3 from concentrations of 5–100 μM in ethanol.

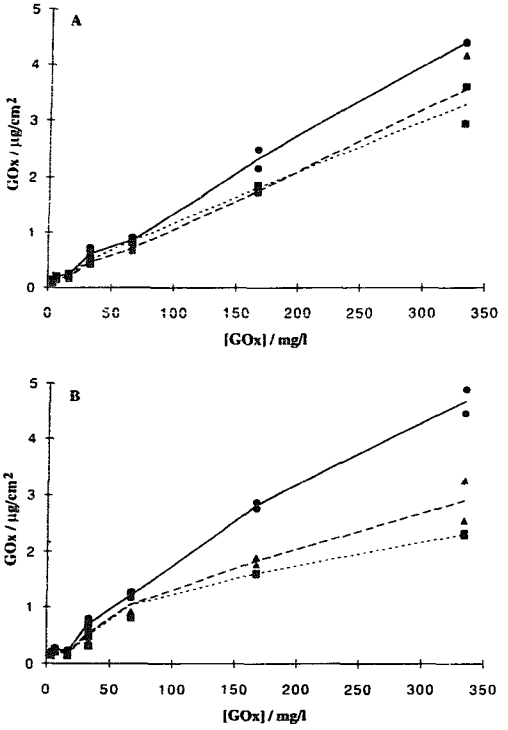

Fig. 5. Binding of glucose oxidase (GOx) to PT2/ODM/Au (A) and PT3/ODM/Au (B) as a function of concentration of enzyme. (——● ——) initially adsorbed; (-▲-) after 2 days desorption in buffer; (-■-) after 15 days desorption in buffer.

mV (vs. Ag|AgCl) in neutral phosphate buffer; the adsorption of ODM causes the stripping wave to be shifted to more positive potential by 300–400 mV. Thus the alkylsulphide functions here as a strong protective coating. When PT2 was adsorbed onto the ODM layer, this barrier to stripping was effectively cancelled, indicating restored electrochemical contact with the electrolyte solution.

3.2. Enzyme adsorption

Both GOx and ChOx were adsorbed onto gold surfaces, modified either with PT2 or PT3, and the amount of enzyme adsorbed determined as described above, using ^{125}I-labeled enzymes. The resulting adsorption isotherms displayed evidence of an indentation in the low concentration region (Figs. 5 and 6). For GOx the indentation was lying at about 17 mg l^{-1} and for ChOx the indentation was less pronounced at about 33 mg l^{-1}. At this point the surface concentration for GOx is roughly in agreement with the estimate of 300 ng cm^{-2} for a monolayer, as calculated via the Stokes' radius. The surface concentration of enzymes continued to rise with concentration up to 330 mg l^{-1} resulting in rather large loadings. For GOx on the PT2-modified electrode about 4 µg cm^{-2} was achieved and for ChOx on the same substrate the value was even higher (6.0 µg cm^{-2}). The electrodes modified with PT3 initially adsorbed much larger amounts of enzyme but the desorption was noticeably larger in comparison with the PT2-modified electrodes. The desorption in buffer is generally most prominent during the first two days at the highest adsorption concentrations. In these cases, however, the amount of enzyme remaining after long periods of desorption was much larger than that expected for a monolayer. The stability of binding was thus quite sufficient.

The adsorption behavior of the two enzymes from a low concentration (33 mg l^{-1}) as a function of molecular wire adsorption concentration was also studied (Figs. 7 and 8). The amount of GOx bound to the PT2-modified ODM/Au (Fig. 7(A)) displays a maximum at around 50 µM PT2 and then slowly decreases when reaching the 200 µM PT2. This may indicate that there is some cooperativity in binding of the (negatively charged) GOx to the positively charged PT2/ODM film at only partial surface coverage of the PT2. GOx binds to the PT3 film in quite a different way (Fig. 7(B)). A depression of the bound enzyme at the 50 µM concentration is observed, indicating a phase of

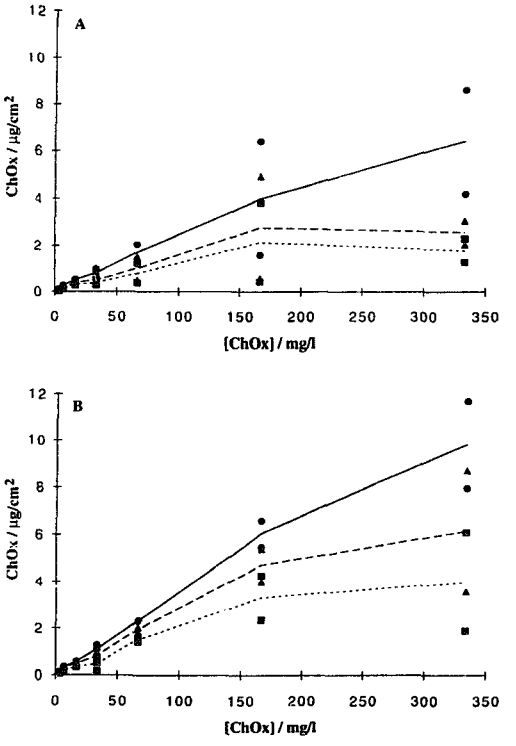

Fig. 6. Binding of choline oxidase (ChOx) to PT2/ODM/Au (A) and PT3/ODM/Au (B) as a function of concentration of enzyme. (——● ——) initially adsorbed; (-▲-) after 2 days desorption in buffer; (-■-) after 7 days desorption in buffer.

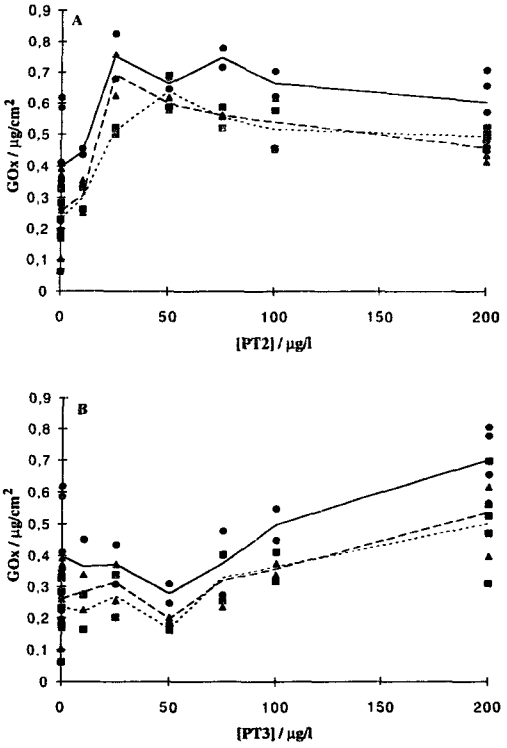

Fig. 7. Binding of glucose oxidase (GOx) to PT2/ODM/Au (A) and PT3/ODM/Au (B) as a function of concentration of conductor. (——●——) initially adsorbed; (-▲-) after 2 days desorption in buffer; (-■-) after 15 days desorption in buffer.

exclusion. The amount of GOx then gradually increases when reaching the 200 µM concentration of PT3. The same types of measurements are given for ChOx in Fig. 8. Here also a clear maximum of binding is observed for the enzyme at 50 µM of PT2, followed by a steady increase of binding till 200 µM. With PT3 the binding initially goes down and then rises. Thus, the surface density of wire has a definitive influence on the enzyme binding and both enzymes behave roughly similarly in this respect.

GOx displayed enzymatic activity, as measured by the spectrophotometric assay, when immobilized onto the ODM/conductor gold electrodes. The activity was most prominent on the slides coated with PT2: 50% of the slides showed an activity higher than 700 µU. With PT3 only 20% of the slides had a similar activity. The results of activity measurements of GOx were, however, highly variable and no clear dependence could be found on the density of the conductor. ChOx showed no enzymatic activity on any electrode. In comparison, ChOx also did not show activity when adsorbed onto polystyrene (Nunc immmunoplate with medium binding capacity), while glucose oxidase was active on this surface. The deactivation of choline oxidase may thus be due to the high hydrophobicity of the alkylated gold surface.

To test the feasibility of complex formation of the His117Gly mutant of azurin with substituted pyridines, we selected two water soluble pyridines (3-(3-pyridyl)-propanol and 3-(4-pyridyl)propanol) as ligands. In the absence of ligand the engineered azurin in the oxidized state exhibits two strong absorption bands at 420 and 628 nm. (Fig. 9, trace 1), which gives the protein solution a green appearance. The Cu(II) in this state is coordinated by His46, Cys112 and two oxygen donors (water and/or hydroxide, depending on pH). At this stage it cannot be excluded that the Cu(II) also has a weak interaction with the sulphur of Met 121. The two absorption bands correspond with the two charge-transfer transitions involving the Cys112 residue and the Cu(II) site. Upon the stepwise titration of the His117Gly(H2O) with either ligand, the absorption spectrum of the copper protein is replaced by a new absorption spectrum exhibiting a single strong band at 635 or 632 nm, for the different ligands (Fig. 9). Accordingly a colour change of the solution from green to deep blue is observed. From previous experiments with a collection of other ligands, including a whole variety of imida-

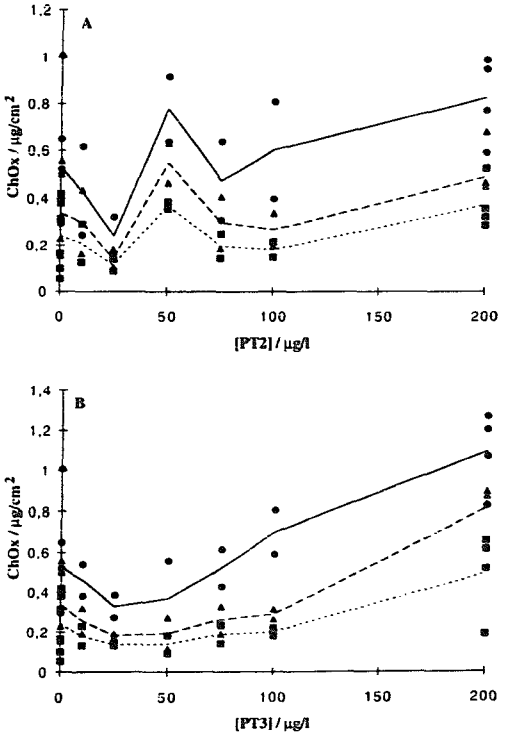

Fig. 8. Binding of choline oxidase (ChOx) to PT2/ODM/Au (A) and PT3/ODM/Au (B) as a function of concentration of conductor. (——·——) initially adsorbed; (-▲-) after 2 days desorption in buffer; (-■-) after 7 days desorption in buffer.

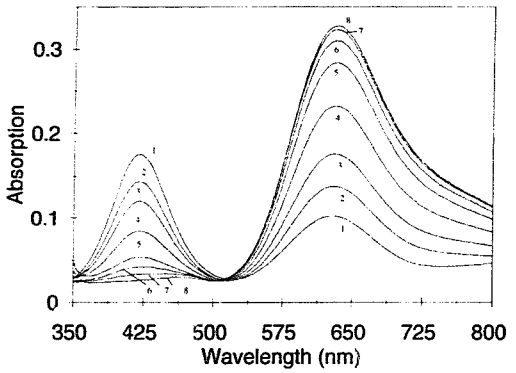

Fig. 9. UV–vis spectra of 75 μM H117G Azurin (20 mM MES buffer, pH 6.0) in the presence of various amounts of 3-(4-pyridyl)-propanol. Concentrations of 3-(4-pyridyl)-propanol amount to 0, 17, 34, 67, 134, 264, 331, and 587 μM (traces 1 to 8).

zole derivatives, it is known that the change in colour is due to the binding of the added ligand and a concomitant change in the coordination of the Cu(II) [22]. In the present case (pH 6.0) the spectral change is due to replacement of one or two waters coordinated to the Cu by a pyridine ligand, which most likely coordinates with its ring nitrogen to the Cu. We also observed that moving the propanol group from the meta- to the para-position of the pyridine decreased the dissociation constant by 1–2 orders of magnitude (from 1.5 ± 0.5 mM to 70 ± 20 μM, respectively).

4. Conclusions

The impedance and electrochemical measurements and the observation that the formed layers were stable and hydrophobic, clearly demonstrate the intrinsic nature of conductivity induced by PT2 and PT3 in self-assembled layers of octadecylmercaptan on the gold surface. Additionally, the shape of the curves in Fig. 3 suggest a Langmuir-type adsorption isotherm for both molecular wires. In their adsorption the electronic link was achieved at a slightly lower adsorption concentration for PT2, which could refer to either a larger affinity of the PT2 for the ODM layer or a mode of incorporation that more effectively enables electronic contact. It also appears that some increase in packing density of the thienoviologens still occurs at concentrations above 50 μM, such that more effective electron transport occurs in CV measurements (Fig. 4). This is also indicated by the gradual changes that are observed in the enzyme adsorption as a function of molecular wire doping concentration. When considering the hydrophobic nature of the surfaces produced and the low values for ϕ at the highest adsorption concentrations, the fractional surface coverage of the thienoviologens may still be quite small.

In general the thienoviologens seem to work as glue between the enzymes and the ODM layer, because the adsorption is always higher in the presence of the molecular wires. This may be due to an electrostatic component being added to the enzyme adsorption, the positively charged pyridinium end groups interacting with negative residues on the protein. The desorption in buffer solution was generally stronger for PT3-modified electrodes, which may yet indicate a lower binding strength of the PT3 to the ODM/gold surface.

The adsorption of the enzymes as a function of thienoviologen adsorption concentration also clearly reveal interesting differences when going through the 10–50 μM adsorption concentration region (where the impedance spectra show their characteristic decrease). A local maximum is observed in the association of both enzymes with the PT2 layer and a local minimum with the PT3 layer. When these results are viewed in the light of structural differences between PT2 and PT3, the former being mono-methylated and the latter dimethylated, it is plausible to assume the hypothesis that their orientations in the ODM layer significantly differ. PT2, with a molecular length of 15 Å, is more suitable to anchor in the approximately 24 Å thick ODM layer in a perpendicular fashion via the unsubstituted pyridine, while the oligothiophene unit of the PT3 must rearrange to a horse-shoe conformation to anchor in the ODM layer via a curved hydrophobic thiophene residue (as illustrated in Fig. 10). In this fashion PT3 may be bound much less tightly than PT2 and may introduce relatively more positive charge, with an orientation less favourable for effective electron transport. In this stage the possibility of formation of mixed monolayers of thienoviologens and ODM, in which the thienoviologens partly displace the ODM layer, cannot be completely excluded. In the light of earlier studies [11,13,14], however, such a situation seems improbable, mainly due to the high irreversibility of the gold-thiolate bond, the low accessibility of the ODM-coated gold surface for the (rather bulky) thienoviologens, and the low concentrations of

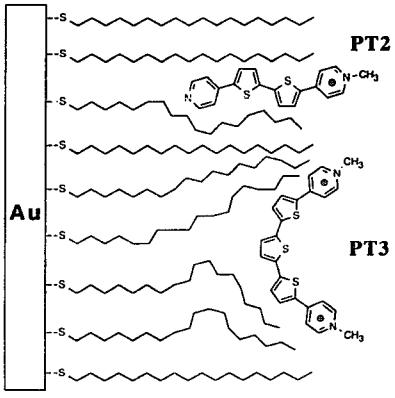

Fig. 10. Proposed modes of interaction of PT2 and PT3 with the ODM layer.

thienoviologens used. The assessment of the amounts of PT2 and ODM on gold substrates as a function of PT2 adsorption concentration with mass spectroscopic techniques, such as secondary ion mass spectroscopy (SIMS), is presently in progress.

The experiments also showed that the concept of constructing self-assembled enzyme electrodes is feasible, because the enzyme layers appeared to be very tightly bound and the molecular wires improved the binding of the enzymes to the gold surface. Additionally, glucose oxidase showed enzymatic activity after 2 weeks preservation in buffer solution. In this respect glucose oxidase appeared to be far more durable than choline oxidase, the latter showing a rapid denaturation both on ODM/gold and polystyrene surfaces.

Finally, successful binding of a spacer with a pyridine end group to an engineered blue copper site appears to be possible, but the binding constant is very sensitive to the structural details of the pyridine group. Moving the propanol group from the meta- to the para-position of the pyridine decreases the dissociation constant by 1–2 orders of magnitude (from 1.5 ± 0.5 mM to 70 ± 20 μM, respectively). Clearly steric factors dictated by the shape of the substituent and the particular shape of the protein channel are decisive factors for obtaining a stable bond.

Acknowledgements

Generous financial support from VTT Chemical Technology is gratefully acknowledged. Part of this work has also been subsidised by the ABON (Association of Research Schools in Biotechnology, The Netherlands). We also express our thanks to Philip Evans (Cranfield Biotechnology Centre) for technical assistance, Ilkka Suni and Hannu Kattelus (VTT Electronics, Otaniemi, Finland) for providing the gold substrates, Petri Vuoristo (Tampere University of Technology) for assistance with the r.f. argon plasma etching and Aulis Marttinen (Tampere University Hospital) for radiolabelling the enzymes.

References

[1] B.A. Gregg and A. Heller, Anal. Chem., 62 (1990) 258.
[2] P.N. Bartlett and J.M. Cooper, J. Electroanal. Chem., 362 (1993) 1.
[3] P.G. Edelman and J. Wang (Eds.), Biosensors and Chemical Sensors, ACS Symposium Series, Publ. No. 487, American Chemical Society, Washington, DC, 1992.
[4] G. Gilardi, T. den Blaauwen and G.W. Canters, J. Contr. Rel., 9 (1994) 231.
[5] T.S. Arrhenius, M. Blanchard-Desce, M. Dvolaitsky, J.-M. Lehn and J. Malthete, Proc. Natl. Acad. Sci. USA, 83 (1986) 5355.
[6] J.P. Launey, S. Woitellier, M. Sowinska and M. Tourrel in F.L. Carter, R.E. Siatkowski and H. Wohltjen (Eds.), Molecular Electronic Devices, Elsevier Science, Amsterdam, 1988, p. 171.
[7] K. Takahashi, T. Nihira, K. Akiyama, Y. Ikegami and E. Fukuyo, J. Chem. Soc. Chem. Commun., 92 (1992) 620.
[8] R. Nakajima, H. Iida and T. Hara, Bull. Chem. Soc. Jpn., 63 (1990) 636.
[9] R. Nakajima, T. Ise, Y. Takahashi, H. Yoneda, K. Tanaka and T. Hara, Phosphorus, Sulfur, Silicon, 95–96 (1994) 535.
[10] K. Takahashi, Jpn. Patent 668277, Sony Corp, Japan, Publ. 23.03.1993.
[11] C.D. Bain, E.B. Troughton, Y.-T. Tao, J. Evall, G.M. Whitesides and R.G. Nuzzo, J. Am. Chem. Soc., 111 (1989) 321.
[12] M.J. Eddowes and H.A.O. Hill, J. Chem. Soc. Chem. Comun., (1977) 771.
[13] P.M. Allen, H.A.O. Hill and N.J. Walton, J. Electroanal. Chem., 178 (1984) 69.
[14] T. Sagara, K. Niwa, A. Sone, C. Hinnen and K. Niki, Langmuir, 6 (1990) 254.
[15] R. Wilson and A.P.F. Turne Biosens. Bioelectron., 7 (1992) 165.
[16] I. Willner, A. Doron, E. Katz and S. Levi, Langmuir, 12 (1996) 946.
[17] K. Tamao, S. Kodama, I. Nakajima, M. Kumada, A. Minato and K. Suzuki, Tetrahedron, 38 (1982) 3347.
[18] W.M. Albers, G.W. Canters and J. Reedijk, Tetrahedron, 51 (1995) 3895.
[19] H.U. Bergmeyer (Ed.), Methods of Enzymatic Analysis, Vol. 15, VCH, Weinheim, 1984.
[20] M. van de Kamp, F.C. Hali, N. Rosato, A.F. Agro and G.W. Canters, Biochim. Biophys. Acta, 1019 (1990) 283–292.
[21] J.R. MacDonald, J. Schoonman and A.P. J Lehnen, J. Electroanal. Chem., 131 (1982) 77.
[22] T. den Blaauwen and G.W. Canters, J. Am. Chem. Soc., 115 (1993) 1121–1129.